

## Faceting of a quasi-two-dimensional GaAs crystal in nanoscale patterned growth

S. C. Lee,<sup>a)</sup> D. L. Huffaker, and S. R. J. Brueck

Center for High Technology Materials and Department of Electrical and Computer Engineering,  
University of New Mexico, 1313 Goddard SE, Albuquerque, New Mexico 87106, USA

(Received 13 September 2007; accepted 13 December 2007; published online 14 January 2008)

The faceting of a quasi-two-dimensional nanoscale crystal (quasi-2D nanocrystal) grown by metal-organic vapor phase epitaxy is reported. Homoepitaxial selective growth is performed on a 200 nm wide, [110]-directed stripe opening fabricated in a 30 nm thick SiO<sub>2</sub> film atop a GaAs(001) substrate. In the cross section perpendicular to the stripe opening, a selectively grown epilayer is regarded as a quasi-2D nanocrystal, which is close to a hexagonal shape symmetrically surrounded with (111)*B*-, (110)- and (111)*A*-type facets from the top as growth proceeds both vertically and laterally. The resulting faceting is interpreted on the basis of equilibrium crystal shape (ECS). The comparison of the observed crystal shape with theoretical modeling enables the measurement of the relative surface energies of the low index orientations. The ECS of a GaAs 2D crystal under the given growth conditions is proposed. © 2008 American Institute of Physics.

[DOI: 10.1063/1.2830988]

Along with the physical dimension, the geometric shape significantly affects the electronic states of semiconductor nanostructures such as quantum dots or nanowires. With the development of nanoscale lithography techniques, patterned epitaxy of nanostructures is readily available. While patterned epitaxy and the associated faceting have been treated in many articles, a systematic explanation based on equilibrium crystal shape (ECS) has not been reported.<sup>1-6</sup> The pattern scale employed in these earlier studies, which was typically micrometers or larger, means that the faceting is localized near the substrate-mask boundary. Additionally, the thickness and sidewall profile of the mask film used to provide selective epitaxy may impact lateral growth, causing interruption of faceting to ECS. Further, the reported experimental results have not been extensively compared with theoretical models.

This work reports the faceting of a nanostructure homoepitaxially grown in a one-dimensional (1D) stripe opening fabricated on a GaAs(001) substrate by metal-organic vapor phase epitaxy (MOVPE). The growth on this 1D pattern results in a quasi-two-dimensional (2D) nanoscale crystal (quasi-2D nanocrystal) since the growth directions of all the facets are coplanar and perpendicular to the pattern direction. First, we examine the faceting of this GaAs quasi-2D nanocrystal. Next, we compare the growth shape with the ECS of a 2D GaAs crystal built up by modeling and determine the surface energies involved in the faceting. To do so, the Wulff point, which is the reference point for the construction of the ECS, must be determined based on the *observed* quasi-2D nanocrystal.<sup>6</sup> However, the experimental evaluation of the Wulff point is ambiguous even in a 2D crystal unless the surface energies of the participating facets are known. For this reason, the model is combined with experimental data to decide the surface energies of low index orientations. This is the key point of our work. Finally, we discuss the discrepancy between experiment and theoretical ECS and related issues for better understanding of ECS.

The patterning of a 30 nm thick SiO<sub>2</sub> film atop a GaAs(001) substrate was performed by *i*-line interferometric lithography and dry etching.<sup>5</sup> The pattern consisted of 200 nm wide, 1D open stripes directed along [110] with a spacing of 1.26 μm. The narrow opening, shown in the inset of Fig. 1(a), and the thin SiO<sub>2</sub> film are favorable for the early initiation of lateral overgrowth and the associated faceting. Also, the large spacing allows uninterrupted faceting without coalescence between adjacent nanostructures. On this patterned substrate, GaAs was deposited using trimethylgallium (TMG) and arsine at 720 °C. A 500 nm film thickness, calibrated on an unpatterned wide-area substrate and a growth rate of ~0.2 ML/s at a V/III ratio of ~300 were supplied. In MOVPE, every facet can be assumed to be exposed to equal partial pressures of TMG and arsine.

Figure 1 shows a scanning electron microscope (SEM) image of the as-grown sample (a) and a cross sectional transmission electron microscope (XTEM) image (b) of a GaAs nanostructure. As seen in Fig. 1(a), the cross sections of the individual nanostructures are not identical but have similar shapes close to that of Fig. 1(b). The dominant facets generated on the nanostructure during growth are (111)*B*, (110), and (111)*A* types. The width of the as-grown nanostructure is about 580 nm, considerably greater than the original 200 nm stripe opening. Figure 1(b) confirms that lateral growth occurs over the SiO<sub>2</sub> mask in both directions.

The insets of Fig. 1(b) present the magnification of the facets near the top of the nanostructure and around the facet intersections. In the inset at the top, (113)*B*- and (001)-type facets are observed with lengths significantly smaller than those of the dominant facets. On the other hand, no additional facets are generated at the (111)*B*-(110) and (110)-(111)*A* intersections. Thus, the facets on the nanostructure are (001) at the top, (113)*B*, (111)*B*, (110), and (111)*A* types. For convenience, these are categorized into two groups based on their physical dimensions along the nanostructure: major [(111)*B*, (110), and (111)*A*] and minor [(001) and (113)*B*] facets.

<sup>a)</sup>Electronic mail: sclee@chtm.unm.edu.

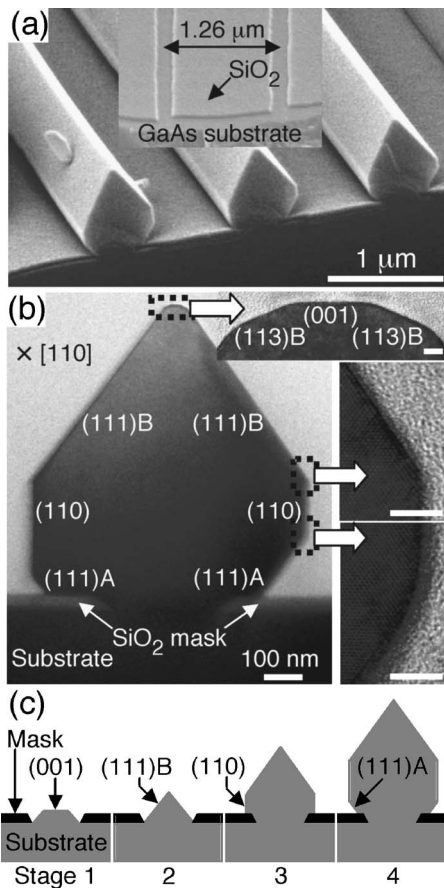


FIG. 1. (a) A SEM image of the as-grown sample. The inset shows a SEM image of the  $\text{SiO}_2$  mask pattern. (b) An XTEM image of a single GaAs nanostructure. The insets provide magnifications of the areas indicated by the dotted boxes. The inset scale bars correspond to 5 nm. (c) A schematic illustration of the major facet evolution.

Based on the reported data and this work, the evolution of major facets on a pattern directed to  $[110]$  is schematically illustrated in Fig. 1(c). The faceting starts with  $(111)B$  resulting in a trapezoidal cross section (stage 1).<sup>1-4</sup> The  $(111)B$  facets extend until the cross section becomes a triangle (stage 2).<sup>1</sup> As growth continues, a  $(110)$  vertical facet is generated at the end of each  $(111)B$  with the initiation of lateral overgrowth (stage 3).<sup>5</sup> With further growth,  $(111)A$  facets appear, as in Fig. 1(b) (stage 4).

The faceting observed in Fig. 1 can be compared with a theoretical ECS. Moll *et al.* and Platen *et al.* have proposed surface energies calculated by density-functional theory.<sup>7,8</sup> Various GaAs orientations have been modeled as a function of the chemical potential of arsenic ( $\mu_{\text{As}}$ ). Figure 2(a) shows the model surface energies of  $(110)$ ,  $(111)A$ ,  $(111)B$ ,  $(113)A$ ,  $(113)B$ , and  $(001)$ . Among the several surface energies for different surface reconstructions, only the lowest surface energy of each orientation is presented in Fig. 2(a) as a function of  $\Delta\mu_{\text{As}} = \mu_{\text{As}} - \mu_{\text{As(Bulk)}}$ . Here,  $\mu_{\text{As(Bulk)}}$  is the chemical potential of arsenic in solid GaAs. For comparison with the model, a value for  $\Delta\mu_{\text{As}}$  under our growth conditions must be determined first. From the minimization of total surface energy and associated geometry shown in Fig. 2(b), the lateral dimension ( $2a$ ) and the length of the  $(110)$  facet  $h_c$  must obey the following relation:<sup>6,7</sup>

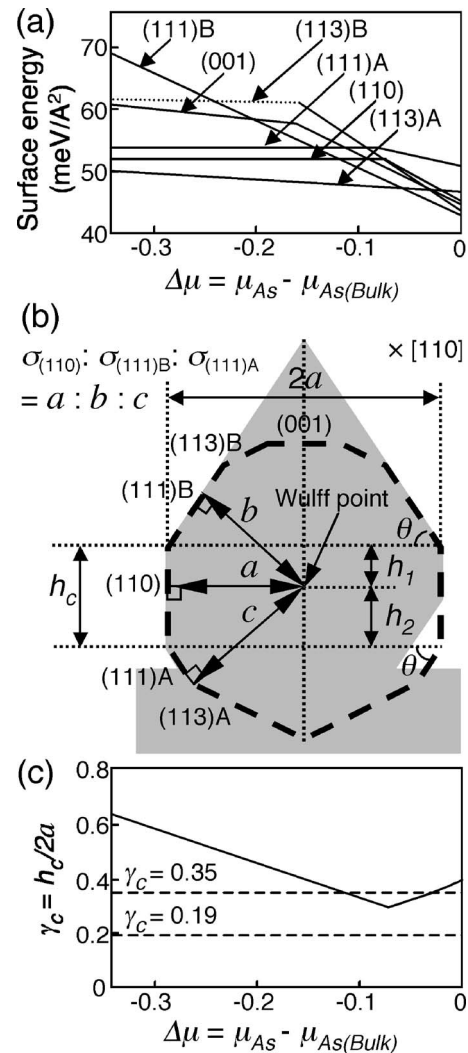


FIG. 2. (a) Calculated GaAs surface energies of various orientations. (b) A schematic replication of Fig. 1(b). The parameters and variables used in Eqs. (1) and (2) are indicated. Due to the asymmetric shape,  $h_1$  and  $h_2$  (or  $h_c$ ) are defined only with respect to the left side which is matched to the model. The bold dashed line represents ECS. (c) A plot of  $\Delta\mu_{\text{As}}$  vs  $\gamma_c = h_c/2a$  defined in Eq. (1).

$$\gamma_c = \frac{h_1 + h_2}{2a} = \frac{h_c}{2a} = \frac{\sigma_{(111)A} + \sigma_{(111)B}}{2\sigma_{(110)} \cos \theta} - \tan \theta, \quad (1)$$

where  $\sigma_{(111)A}$ ,  $\sigma_{(111)B}$ , and  $\sigma_{(110)}$  are the respective surface energies and  $\theta = 54.7^\circ$ . The solid line of Fig. 2(c) corresponds to  $\gamma_c$  of Eq. (1) calculated from the surface energies given in Fig. 2(a). Experimentally, the asymmetric cross section has two different  $\gamma_c$ 's,  $\sim 0.35$  for the left side and  $\sim 0.19$  for the right side when  $a \sim 290$  nm.<sup>9</sup> In Fig. 2(c), as indicated by dashed lines, only the  $\gamma_c$  of the left side can match the model. The asymmetric cross section resulting in two different  $\gamma_c$ 's from a single cross section is partly due to the extrinsic effects such as the profile and thickness of the  $\text{SiO}_2$  mask. This limitation on ECS study will be discussed later. Assuming that the left side is close to ECS under the given growth conditions,  $\Delta\mu_{\text{As}} \sim -0.12$  and  $-0.03$  are obtained from Fig. 2(c). Both of these values are on the As-rich side, consistent with our experimental conditions.<sup>7</sup> However, it is questionable if MOVPE can provide a sufficient arsenic partial pressure to reach the condition of  $\mu_{\text{As}} \sim \mu_{\text{As(Bulk)}}$ . That is, the condition of  $\Delta\mu_{\text{As}} = -0.03$  may not be attainable in a

TABLE I. Ratios of experimental and theoretical surface energies of various orientations to that of (110) in GaAs.  $\sigma_{(110)}$  is taken to be 52.0 meV/Å<sup>2</sup>.

	(111) <i>B</i>	(111) <i>A</i>	(001)	(113) <i>B</i>	(113) <i>A</i>
Ratio to $\sigma_{(110)}$	1.00	1.04	1.05(mod)	1.08(mod)	0.93
			1.57(exp)	1.45(exp)	(mod)

growth reactor with a restricted arsine supply capability. For this reason, the surface energies at  $\Delta\mu_{\text{As}}=-0.12$  are more relevant than those at  $\Delta\mu_{\text{As}}=-0.03$  for the faceting of Fig. 1(b). Then, as indicated in Fig. 2(b), the Wulff point for  $\Delta\mu_{\text{As}}=-0.12$  can be determined from<sup>6,7</sup>

$$\frac{h_1}{h_2} = \frac{\sigma_{(111)B} - \sigma_{(110)} \sin \theta}{\sigma_{(111)A} - \sigma_{(110)} \sin \theta} \sim 0.8. \quad (2)$$

Here,  $h_1$  and  $h_2$  are positive for given growth condition. Table I summarizes the surface energies of all the facets involved in Fig. 1(b) which are obtained from the Wulff point using the relationship indicated in Fig. 2(b).

As mentioned earlier, the determination of the Wulff point for an observed shape is the key point of this work. Using Eq. (1), the experimental data ( $\gamma_c=0.35$ ) is coupled to the surface energies of the *major* facets at  $\Delta\mu_{\text{As}}=-0.12$  of the modeling. For this reason, every major facet in Table I has a unique surface energy ratio for this geometry. The surface energy ratios of (111)*B* and (111)*A* to (110) are 1.00 and 1.04, respectively. Thus, the surface energy of (111)*B* is identical with that of (110) and slightly less than that of (111)*A*. As noted in Fig. 2(a), these are valid around  $\Delta\mu_{\text{As}}=-0.12$  in the model even when the variation of the observed  $\gamma_c$  is considered. Despite the phenomenological approach used in this work, this result is qualitatively consistent with our previous work.<sup>10</sup>

The bold dashed line of Fig. 2(b) represents the ECS of a GaAs 2D crystal conjectured from Table I. If the model is correct, the cross section of Fig. 1(b) is not ECS. According to Fig. 1(c), the crystal shape depends on the deposition amount in nanoscale patterned growth. Although the shapes from stages 1 to 4 are not ECS, it is clear that the shape evolves to ECS as the growth proceeds. The sequential formation of (110) and (111)*A* along the bold dashed line provides strong evidence that the nanostructure is being driven to the ECS shown in Fig. 2(b) by dynamical faceting. This is a very important result supporting the surface energies of the major facets listed in Table I in spite of the discrepancy of the experimental cross section from the conjectured ECS. At stage 4 of Fig. 1(c), the nanostructure will keep this shape in continued growth until other facets such as (001) and (113)-type orientations are available as major facets.<sup>11</sup>

In Figs. 1(b) or 2(b), the cross section is not symmetric. The uneven lateral overgrowth accompanying this asymmetric shape is mainly a result of the fluctuations in the sidewall profile and thickness of the SiO<sub>2</sub> mask at the substrate-mask boundaries which inevitably arise in nanoscale lithography and etching. Energetically, the lateral overgrowth could be encouraged more easily with the formation of vertical (110) facets than of (111)*B* facets which form an obtuse angle with the mask. Then, the extended (111)*B* at stage 2 of Fig. 1(c) could be due to the physical suppression of lateral growth by the mask film. Such an extension may require the interpolation of (001) and (113)*B* orientations between (111)*B* facets

at the top. This means that the discrepancy in the minor facet surface energies of Table I includes these effects. As seen in Fig. 2(a), the surface energies widely vary with  $\Delta\mu_{\text{As}}$ , and are affected by growth temperature and arsine vapor pressure. Some surface reconstructions assumed in the model may not be available at our growth temperature. However, it must be emphasized that this work focuses on an analytical method to measure these energies and to predict shape evolution with ECS and theoretical modeling.

Further study is required to understand surface energies and correlated faceting with the variation of growth parameters. Extrinsic effects on faceting associated with the presence of the SiO<sub>2</sub> mask imply that the ideal ECS shown in Fig. 2(b) may not be proven simply by continued growth. Also, the interface energy between the SiO<sub>2</sub> mask and the GaAs epilayer must be considered in the shape analysis.<sup>5</sup> Nonetheless, our approach provides reliable data because the cross section of the epilayer in Fig. 1(b) has a height and a lateral dimension considerably greater than the stripe opening width. Unlike previous work,<sup>1-4</sup> this implies more degrees of freedom for the faceting, which should be less affected by the SiO<sub>2</sub> mask as growth proceeds. Furthermore, the cross section already includes the low-surface-energy facets, as the major facets valid for ECS. For these reasons, the results of this work suggest strong possibility of ECS study relying on nanoscale patterned growth and of the predictable shape control of nanostructures which are very important to semiconductor nanoscience and nanotechnology.

In conclusion, the relative surface energies of (110), (111)*B*, and (111)*A* of GaAs selectively grown on a 200 nm wide stripe opening by MOVPE have been measured with ECS and a theoretical model. The surface energy ratios of (111)*B* and (111)*A* to (110) are  $\sim 1.00$  and  $\sim 1.04$  at our growth condition. The experimental data suggest that the shape of an epilayer evolves to ECS with dynamical faceting during nanoscale patterned growth.

The support for this work was provided by DOE under subcontract from Sandia National Laboratories.

<sup>1</sup>K. Kamon, S. Takagishi, and H. Mori, *J. Cryst. Growth* **73**, 73 (1985).

<sup>2</sup>T. Kuech, *J. Cryst. Growth* **115**, 52 (1991).

<sup>3</sup>L. Korte, Chr. Thanner, M. Huber, and Ch. Hoyler, *J. Cryst. Growth* **124**, 220 (1992).

<sup>4</sup>K. Shimoyama, N. Hosoi, K. Fugii, and H. Gotoh, *J. Cryst. Growth* **145**, 283 (1994).

<sup>5</sup>S. C. Lee, L. R. Dawson, and S. R. J. Brueck, *Appl. Phys. Lett.* **87**, 071110 (2005).

<sup>6</sup>For details of ECS, see, for example, M. Wortis, in *Chemistry and Physics of Solid Surfaces*, edited by R. Vanselow and R. F. Howe (Springer, Berlin, 1988), Vol. VII, p. 367.

<sup>7</sup>N. Moll, A. Kley, E. Pehlke, and M. Scheffler, *Phys. Rev. B* **54**, 8844 (1996).

<sup>8</sup>J. Platen, A. Kely, C. Setzer, K. Jacobi, P. Ruggerone, and M. Scheffler, *J. Appl. Phys.* **85**, 3597 (1999).

<sup>9</sup>In XTEM, 14 cross sections similar to Fig. 1(b) were examined. Every two  $\gamma_c$ 's from each cross section were classified into two groups, a large  $\gamma_c$  to group 1 and a small  $\gamma_c$  to group 2. The average of group 1(2) was 0.35 (0.22). Although some fluctuation was observed in both groups, 6 out of 14  $\gamma_c$ 's were within  $\pm 5\%$  from 0.35 in group 1. The cross section in Fig. 1(b) has been chosen for this article since  $\gamma_c$  on the left side coincides with the average of group 1 while that on the other side does not affect conclusion.

<sup>10</sup>S. C. Lee, L. R. Dawson, and S. R. J. Brueck, *J. Appl. Phys.* **96**, 1214 (2004).

<sup>11</sup>For example, the formation of (113)*A* orientation can be examined by changing the pattern direction from [110] to  $[1\bar{1}0]$ .